CONTROL OF CONVECTIVE THERMAL EXCHANGE IN A LAVAL NOZZLE DURING TURBULENT FLOW WITH A LOCAL SEPARATION ZONE

E. G. Zaulichnyi and V. M. Trofimov

UDC 536.24:532.54

Separation and combining of supersonic flows often occurs in elements of contemporary high-energy devices. Many studies have been made on flow around projections, cavities, and angular configurations [1-7]. Because of the difficulties of developing methods for determining convective turbulent thermal exchange in similar flows, detailed experimental investigations must be conducted.

The purpose of the study is to determine the effect on flow and heat exchange of a change in the form of a cavity with a projection placed against the flow. The cavity is situated on the wall of a Laval nozzle, i.e., there is internal streamline flow with a negative pressure gradient.

Experiments have been done on a horizontal jet system [8]. The experimental model is a planar nozzle with a width of 32 mm and with two cavities on its generatrix symmetrically placed relative to the axis. One of the cavities is shown in Fig. 1a, where h_1 and h_2 are the heights of the vertical walls of the cavity toward and against the flow. Pressure transmitters are located on one generatrix and a thermal exchanger is located on the other. The cone half-angle of the nozzle is 24°, $h_1 = 7.5$; 12 mm, $h_2 = 6$ mm. The length of the cavity L may be varied from 0 to 67 mm. The boundary layer in front of the separation region is turbulent. The measured thickness of the boundary layer directly in front of the cavity is $\delta_1 = 2$ mm, the Mach number in front of the separation is $M_1 = 2.6$, and the Reynolds number, which was determined across the critical cross section of the nozzle in experiments, is $5 \cdot 10^6$. The gas parameters (for air) in the antechamber of the nozzle are as follows: the pressure is $p_0 = 1.0$-1.3 MPa, and the stagnation temperature is $T_0 = 255$-270 K.

Shadow diagrams with microsecond exposures allow one to detect, as was done in [7], insignificant "vibration" of a system of discontinuities with amplitudes much less than the average thickness of the displaced layer. For $L/h_1 = 3.5$, a system of discontinuities is observed related to instability in the flow apparently due to some type of hysteresis.

The local heat-exchange coefficients under quasisteady-state conditions of flow are measured using the specially developed methodology in [9], which is valuable for making measurements of heat exchange in supersonic flows under complex conditions [8]. This method involves using a small electric preheater of graphite film mounted with glue in the form of a rectangle along the channel wall. Thermocouples are mounted flush with a wall made of a insulating material along the axis of the rectangle under the film and their signals are passed into the memory of a microcomputer. The time resolution of this method allows for sensitivity to nonsteady-states with a frequency above 5 Hz. Under experimental conditions, heat loss in the wall is no more than 1.5% of that input into the film. Total losses in the nozzle unrelated to convective heat exchange are no greater than 2%. Nonuniformity of the film over its thickness is accounted for by calibrations made before and after the experiment under any conditions. The electrical resistance of the film is controlled over the duration of the experiment and has no impact on the measurement results. Measurement of the pressures on the walls of the model are done with the GRM-2 group registration manometer with working ranges of -0.1... $+0.1$ and -0.1... $+0.7$ MPa. The response time of the instrument under experimental conditions is determined by the volume of the pneumatic path and is on the order of a few seconds. The accuracy class of the GRM-2 is 0.5.

Obtained shadow diagrams with microsecond exposures (Fig. 1) indicate the characteristic states of flow around the cavities. On the flow schematic (Fig. 1a) constructed from the photographs (Fig. 1b), one may find the state corresponding to a closed cavity. It is evident that the boundary layer, which separates from the

Novosibirsk. Translated from Zhurnal Prikladnoi Mekhaniki i Tekhnicheskoi Fiziki, No. 3, pp. 110-115, May-June, 1987. Original article submitted March 28, 1986.

0021-8944/87/2803-0418$12.50

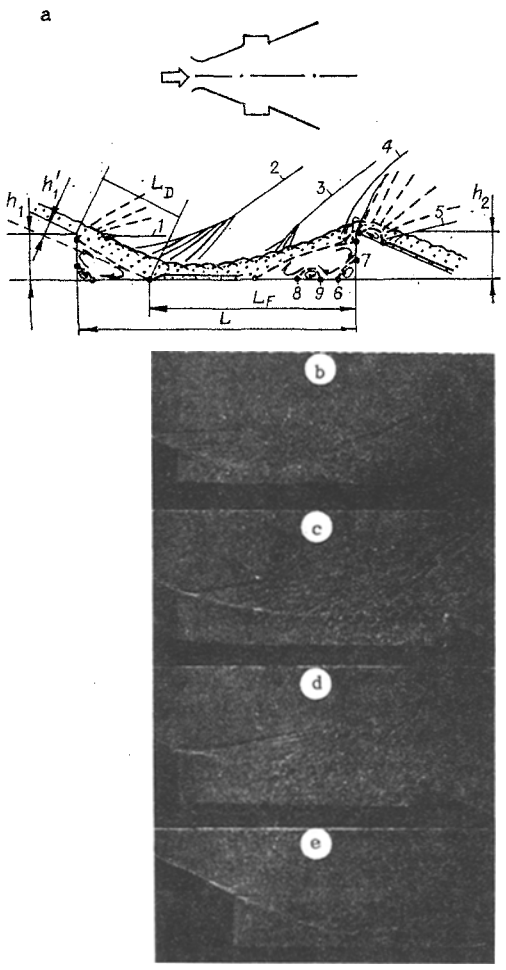

Fig. 1

leading edge of the cavity, expands and combines with the horizontal wall of the cavity. Hence, a region of reduced pressure is closed off near the leading wall of the cavity, while a boundary discontinuity 1 sits on the edge due to overexpansion. Near the region where the boundary layer becomes attached, an intense discontinuity 2 arises, and the flow rotates and moves along the walls of the cavity forming a wide region of highly turbulent flow. A discontinuity arises in front of the trailing wall of the cavity and forms a closed separation region of compression, where one observes the separation discontinuity 3, and the discontinuity 4 is separated in front of wall h_2. Attachment of the boundary layer does not occur at its edge but somewhat earlier on wall h_2. This was indicated in [3] in experiments conducted on external flow around a step. Because of attachment to wall h_2, which is against the flow, part of the gas in the boundary layer perpendicular to the external high-velocity flow rotates. As a result, a separation region with a size on the order of δ_1 appears in the flow, which is evident in the shadow diagrams (Fig. 1b-d). Expansion occurs beyond the edge of the cavity (up to overexpansion of the flow) with the formation of a boundary discontinuity 5, after which the pressure is restored.

If L/h_1 is decreased, a new state arises in which a discontinuity is generated after attachment of the boundary layer on the edge of the cavity (Fig. 1c). The discontinuities observed earlier for attachment 2 and separation 3 merge together. For a further decrease in L/h_1, the freely displaced layer (which separates the boundary layer) is forced aside to the flow and the cavity opens (Fig. 1d). In these cases, the displacement layer continutes to grow and the highly turbulent flow expands, while the system of shock waves are pushed aside into the flow from the walls of the cavity.

For flow around a cavity without an opposite projection (Fig. 1d), a closed expansion region is formed, there is a boundary discontinuity near the separation region, and there is an intense attachment discontinuity in the attachment region. For the states indicated in Fig. 1b-e, it is evident that the large vortices formed in the freely displaced layer reach the walls of the cavity, while this does not occur for others.

The pressure distributions on the cavity wall without the projection against the flow, on the nozzle wall, on the walls of a cavity with a projection against the flow, and on the walls of the nozzle beyond the cavities

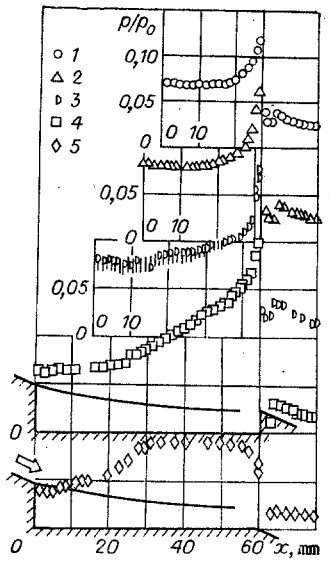

Fig. 2

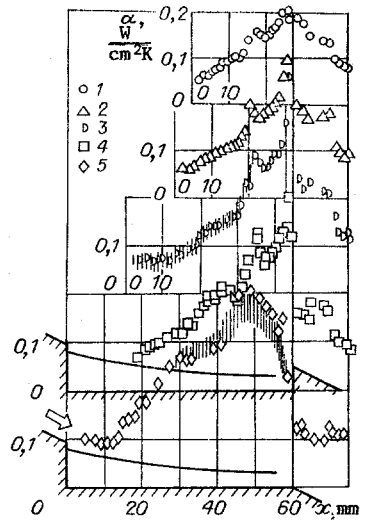

Fig. 3

are indicated in Fig. 2 [5] $h_1 = 12$ mm, $h_2 = 0$, $L = 60$ mm, while in the remaining cases, $h_1 = 12$ mm, $h_2 = 6$ mm, $L = 27$; 31.5; 44.5; 60 mm (points 1-4)].

Local heat exchange coefficients α indicated in Fig. 2 are represented in Fig. 3 ($p_0 = 1.2$ MPa, $T_0 = 261$ K). The data are situated so that the trailing wall of all the cavities are along a single vertical. The Mach numbers before the separation from the leading edge of the cavity are equal ($M_1 = 2.6$). The pressure distribution and the heat exchange on the wall of a closed cavity with a projection against the flow are shown in Fig. 4, where $h_1 = 7.5$ mm, $h_2 = 6$ mm, and $L = 67$ mm.

A comparison of the pressure distributions on the wall of the cavity without the projection against the flow (Fig. 2, curve 5) and the closed cavity with the projection (Fig. 4, curve 2) indicates that they coincide with the region where the flow expands after separation from the leading edge of the cavity and in the region of attachment to the horizontal wall of the cavity. After attachment (Fig. 2, curve 5), the pressure is constant before the edge of the cavity and then sharply decreases on the nozzle wall. In Fig. 4, curve 2, the pressure begins to rapidly grow before the projection against the flow, and separation then occurs. Hence, a local maximum is found in the separation zone, and the pressure sharply increases up to a second maximum in a narrow region before the projection. The nonmonotonic character of the pressure distribution in the compression region before the projection is due to the intense recirculation of the flow and to the presence of discontinuity 3 (see Fig. 1a). The high relative level of the pressure maxima in this region in comparison with external flow around a step [1, 3] is related to peculiarities in the internal flow. For an estimate of the increase in the pressure in the attachment regions of the cavity, a one-dimensional calculation was made for a nozzle without a cavity and is shown (with a line) in Fig. 2.

When L/h_1 is decreased ($h_2 = 6$ mm remains constant), the flow is restructured (Fig. 2, curve 4), and the separation regions for expansion near the wall h_1 and compression near the wall h_2 begin to combine. The critical length of closure of the cavity for a given nozzle cone half-angle $L_{cr}/h_1' = (L_D/h_1') + (L_F/h_2)[h_2/h_1'] = 14$ is greater than the total length of the closed regions of expansion and compression. Evidently, this is related to the appearance of a type of hysteresis, which has been observed in aerodynamic flows. A further decrease in L/h_1 leads to equalization of the pressure gradients longitudinal with respect to the perimeter of the cavity (Fig. 2, curves 1-3). The pressure decreases near the trailing wall of the cavity but increases near the leading edge, which agrees with the experimental data from [10, 11] obtained for external flow around a rectangular cavity. When $L/h_1 = 3.6$ (Fig. 2, curve 3), relative instability is observed in the pressure distribution (indicated with the dashed lines), which is determined by the deviation of the experimental points from the average position.

A faster increase is observed in the distribution of local heat exchange coefficients in the attachment region to the horizontal wall without the projection (Fig. 3, curve 5) in comparison with a closed cavity with a projection (Fig. 4, curve 1). Hence, the intensity of heat exchange is two to three times greater than the calculated values for a nozzle without a cavity (curves in Fig. 3) obtained with the method in [12]. The time resolution of the measurements of the local heat exchange coefficients allows one to determine the relative non-

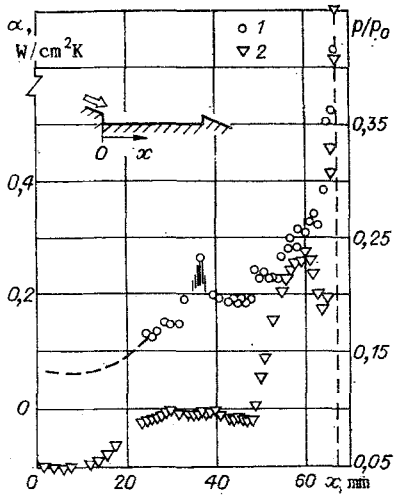

Fig. 4

steady-state character of the heat exchange coefficients with a scale of 1-5 Hz in the narrow region of the maximum, which is defined by the vertical dashed line for the cavity (Fig. 4, curve 1) and in a wide range for the cavity (Fig. 3, curve 5). The amplitude of the oscillations is on the order of 15% of the average value of the heat exchange coefficients. Evidently, the nature of heat exchange in these cases is affected by perturbations generated by the system of discontinuities in the separation region. Near the repeated separation of the boundary layer before the projection (Fig. 4, curve 1), heat exchange is increased by the discontinuity before some constant level and then increases past the bend up to the maximum values directly near wall h_2.

When L/h_1 is decreased, the cavity opens, and the heat exchange coefficients decrease in the region in front of wall h_2 (Fig. 3). In the region attached to wall h_1 of the cavity, a decrease in L/h_1 does not lead to an increase in the pressure due to heat exchange (Fig. 2), but the pressure is kept constant at about 40% below the calculated curve (Fig. 3), obtained for a nozzle without a cavity [12]. A sharp reduction in heat exchange occurs on the wall of the nozzle beyond the cavity, but, in contrast to the pressure, the values of the heat exchange coefficients do not immediately reach a level corresponding to that for a nozzle without a cavity but exceed by about 80% the values for unperturbed flow.

Because of increased turbulence, (see Fig. 1b-d), the presence of two maxima α near wall h_2 of the cavity (Fig. 3, curves 2-5) does not seem to explain the case when $M_\infty = 0.85$ [13] due to a change in the state of the thin boundary layers near the walls from laminar to turbulent. In addition, if there exist two separation zones 6-7 and 8-9 (see Fig. 1a), which appear, for example, during subsonic flow around a step [13], curve 6 corresponds to the first maximum α and curve 8 corresponds to the second. The condition for separation of flow ($dp/dx > 0$) near point 9 is also satisfied for an open cavity because there is a sharp salient point in the pressure distribution curve (Fig. 2, curves 2-5). Regarding the behavior of α, one can conclude that the size of region 6-7 changes over time when $L/h_1 > 2.3$. The second maximum is clearly expressed, and its position is independent of the change in L/h_1 (Fig. 3, curves 3-5). Consequently, the separation zone 8-9 is stable, but its position and size under equivalent conditions are determined by the dimension h_2.

The experimental results indicate that a large-scale nonsteady state occurs only in the transitional state of flow around a cavity for $L/h_1 = 3.6$, when instability is observed with measurements of the pressure and heat exchange over the entire length of the cavity (Fig. 2, curve 3, and Fig. 3, curve 3, the amplitude of the oscillations is indicated with the dashed lines). One may distinguish the nonsteady-state nature of heat exchange in the cases of Fig. 3, curve 5, and Fig. 4, curve 1, which is due to the close proximity of discontinuities 2 and 3 (see Fig. 1a) to the wall and is local.

A change in the geometric form of the cavity has an effect on the heat exchange coefficients and the pressure pertaining to the separation point (Fig. 5, where 1 and 2 are the maximum values of the heat exchange coefficients and pressure, respectively, while 3 and 4 are their minimum values). If for $L/h_1' = 6.7$, the maximum values of α/α_1 and p/p_1 differ by 10%, then for $L/h_1' = 10.6$ the difference is 27%. Therefore, the quantity α/α_1 for all L/h_1' exceeds p/p_1. On the other hand, the minimum values of p/p_1 exceed the minimum values of α/α_1, and both of these quantities are weak functions of L/h_1'.

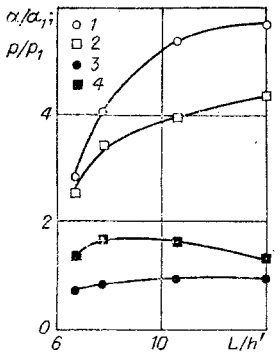

Fig. 5

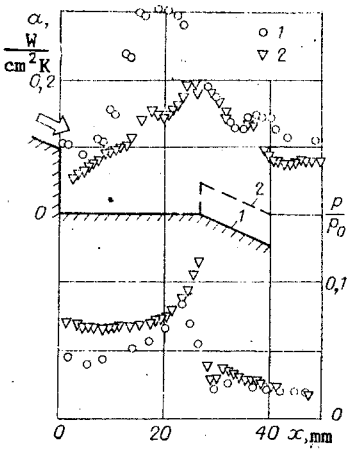

Fig. 6

The pressure and heat exchange distributions on the walls of two types of cavities are shown in Fig. 6: 1) without a projection against the flow ($h_1 = 12$ mm, $h_2 = 0$, $L = 27$ mm), 2) with a projection ($h_1 = 12$ mm, $h_2 = 6$ mm, $L = 27$ mm). It is evident that as the pressure on the wall of the cavity in the first case is less than in the second case, the heat exchange is on the average 1.5 times greater. The pressure distribution on the nozzle wall beyond the cavity is independent of the cavity form, but the heat exchange is dependent and takes on higher values for a cavity without a projection against the flow.

On the basis of experimental data, one can conclude that the primary feature of convective heat exchange in flows with local separation zones is the intensification of its high level of turbulence in the flow attached to the walls. The amount of turbulent transfer is basically determined by large vortices, and the intensity of heat exchange directly depends on the nearness of the layers of large vortices (see Fig. 1a, where arcs near the upper boundary of the viscous surface flow are used to define the vortices) to the heat exchange surface. Consequently, control of the separation flow for decreasing the very high level of heat exchange in the attachment region and in the relaxation section beyond it is possible by changing the geometric form of the cavity. Effective compression of heat exchange in these regions is achieved by pushing large energy-carrying vortices generated near the outer boundary of the freely displaced layer into the flow from the heat exchange surface, and, although the region of intense surface vortex flow increases on the whole (see Fig. 1d, e), only small vortices are observed near the heat exchange surface that accelerate the transition of the flow to an equilibrium state. This external effect on the characteristics of turbulent transfer near the attachment region of the flow can be organized by different means, such as using an intake, a blower, or thermal screens. The method applied in this study (Fig. 6) is very simple and can be used for optimization of the form of distortion on a channel wall.

LITERATURE CITED

1. P. Chang, Separation of Flow, Vols. 1-3, Pergamon (1970).
2. L. V. Gogish and G. Yu. Stepanov, Turbulent Separation Flows [in Russian], Nauka, Moscow (1979).
3. A. A. Zheltovodov, "Analysis of properties of two-dimensional separation flows at supersonic velocities," in: Analysis of Surface Flow of a Viscous Gas [in Russian], Inst. Teor. Prikl. Mekh., Sib. Otd., Akad. Nauk SSSR (1979).
4. A. A. Zheltovodov, É. Kh. Shilein, and V. N. Yakovlev, Evolution of a Turbulent Boundary Layer During Combined Interaction with Compression Discontinuities and Rarefraction Waves, Preprint Inst. Teor. Prikl. Mekh., Sib. Otd., Akad. Nauk SSSR, No. 28-83, Novosibirsk (1983).
5. A. F. Charwat, C. F. Dewey, and J. N. Roos, "An investigation of separated flows. Part II: Flow in the cavity and heat transfer," J. Aerospace Sci., 28, No. 7 (1961).
6. G. S. Settles, B. K. Baca, D. R. Williams, and S. M. Bogdonoff, "A study of reattachment of a free shear layer in compressible turbulent flow," Paper/AIAA, No. 1408, N. Y. (1980).
7. K. Khayakava, A. Smits, and C. M. Bogdonov, "Experimental investigation of the characteristics of turbulence in attached displacement layer in a compressible gas," Aerokosmich. Tekh., 2, No. 12 (1984).
8. E. G. Zaulichnyi and V. M. Trofimov, "Investigation of heat transfer in separation regions for supersonic flow in a Laval nozzle," Zh. Prikl. Mekh. Tekh. Fiz., No. 1 (1986).
9. V. N. Zaikovskii, E. G. Zaulichnyi, et al., "Experimental investigation of local heat transfer coefficients on the walls of a valve system," Zh. Prikl. Mekh.Tekh. Fiz., No. 2 (1982).

10. Emeri, Sadunas, and Lol, "Heat transfer and pressure distribution for flow over a cavity," Teploperedacha, No. 1 (1967).
11. Vestler, Saida, and Okser, "Heat transfer to the surface of steps and cavities in supersonic turbulent flow," Raket. Tekh. Kosmon., No. 7 (1969).
12. S. S. Kutateladze and A. I. Leont'ev, Heat and Mass Transfer and Friction in a Turbulent Boundary Layer [in Russian], Énergiya, Moscow (1972).
13. V. P. Solntsev, B. E. Luzhanskii, and V. N. Kryukov, "Investigation of heat transfer in turbulent separation zones near projections," Teplo. i Massperenos., Inst. Teplo. i Massoobmena, Akad. Nauk Beloruss. SSR, Minsk, 1 (1972).

SPEED AND ATTENUATION OF SOUND IN GAS – VAPOR – LIQUID SYSTEMS. ROLE OF HEAT AND MASS EXCHANGE

D. A. Gubaidullin and A. I. Ivandaev

UDC 534.2:532.529

Several theoretical and experimental papers have been devoted to the study of the propagation of acoustic excitations in one and two-component, two-phase media of the gas suspension type [1-13]. The propagation of small-amplitude acoustic excitations in a mixture of vapor or gas with liquid drops was considered in [1-3]. Excitations of finite amplitude were considered in [4, 5]. The dispersion and absorption of weak sound waves was studied in [6-12] for a mixture of an inert gas with liquid drops and water vapor. The propagation of finite-amplitude excitations in fog was analyzed in [13]. The effect of the unsteady interaction of the phases on the propagation of high-frequency excitations was studied in [2, 3] for single-component mixtures of vapor and liquid drops. In the present paper we study the dispersion and attenuation of sound in one and two-component gas–liquid mixtures.

1. Basic Equations of Motion and Equations of State. We consider monodispersed mixtures and assume acoustic homogeneity. In order to study the phenomena, we use the model of a two-velocity and three-temperature continuum [14]. We consider the linearized equations of motion in the plane, one-dimensional case in the presence of phase transitions. In a coordinate system in which the unperturbed mixture is at rest, the conservation equations of mass and momentum for the phases are

$$\frac{\partial \rho_1'}{\partial t} + \rho_{10}\frac{\partial v_1'}{\partial x} = -nj_{V\Sigma},\ \frac{\partial \rho_V'}{\partial t} + \rho_{V0}\frac{\partial v_1'}{\partial x} = -nj_{V\Sigma},\ \frac{\partial \rho_2'}{\partial t} + \rho_{20}\frac{\partial v_2'}{\partial x} = nj_\Sigma,$$
$$\rho_{10}\frac{\partial v_1'}{\partial t} + \frac{\partial p_1'}{\partial x} + nf = 0,\ \rho_{20}\frac{\partial v_2'}{\partial t} = nf, \tag{1.1}$$
$$\rho_{10} = \alpha_{10}\rho_{10}^0,\ \rho_{20} = \alpha_{20}\rho_{20}^0,\ \alpha_{10} + \alpha_{20} = 1,\ \alpha_{20} = \frac{4}{3}\pi a_0^3 n,$$
$$\rho_1 = \rho_V + \rho_G,\quad p_1 = p_V + p_G,$$

where ρ and ρ^0 are the reduced and true densities; v and p are the velocity and pressure; α is the volume content; n is the number of particles per unit volume; f is the force on an individual liquid drop due to the carrier phase; $j_{V\Sigma}$ is the diffusive flux of vapor to the surface Σ of a drop; j_Σ is the rate of condensation onto the surface of an individual drop. Here and below the subscripts 1 and 2 refer to the gaseous phase and the suspended phase, V and G refer to the vapor and gas components of the carrier phase, and the primes denote small perturbations, while the subscript 0 denotes the initial unperturbed state.

The equations governing the supply of heat to the gaseous phase, to the drops, and to the surface of an individual drop can be written as

$$\rho_{V0}\frac{\partial i_V'}{\partial t} + \rho_{G0}\frac{\partial i_G'}{\partial t} = \alpha_{10}\frac{\partial p_1'}{\partial t} - nq_{1\Sigma},\ \rho_{20}\frac{\partial u_2'}{\partial t} = -nq_{2\Sigma}, \tag{1.2}$$
$$q_{1\Sigma} + q_{2\Sigma} = -j_\Sigma l,$$

Moscow. Translated from Zhurnal Prikladnoi Mekhaniki i Tekhnicheskoi Fiziki, No. 3, pp. 115-123, May-June, 1987. Original article submitted April 7, 1986.

0021-8944/87/2803-0423 $12.50